Journal of Power Sources 196 (2011) 6969–6973

Contents lists available at ScienceDirect

Journal of Power Sources

journal homepage: www.elsevier.com/locate/jpowsour

Short communication

Electrochemical and magnetic studies of Cr^{3+}- or Co^{3+}-substituted Li–Mn–Ni spinel oxides

Naoki Kawai [a], Tatsuya Nakamura [a,*], Yoshihiro Yamada [a], Mitsuharu Tabuchi [b]

[a] Department of Electrical Engineering, Graduate school of Engineering, University of Hyogo, 2167 Shosha, Himeji, Hyogo 670-2280, Japan
[b] National Institute of Advanced Industrial Science and Technology, Osaka 563-8577, Japan

ARTICLE INFO

Article history:
Received 30 September 2010
Received in revised form 30 October 2010
Accepted 3 November 2010
Available online 11 November 2010

Keywords:
High-voltage cathode
Spinel oxide
Magnetic property
Electrochemical property

ABSTRACT

$LiMn_{1.5-x}M_{2x}Ni_{0.5-x}O_4$ (M = Co or Cr, $0.0 \le x \le 0.2$) compounds were synthesized by the sol–gel method. It is found from X-ray diffraction analysis that single spinel phases are obtained for both Cr^{3+}- and Co^{3+}-substitution, but a small cation mixing between the 8a and 16d sites is found only in the Co^{3+}-substitution case. All of the compounds exhibit *M–T* curves characteristic of ferromagnetic materials. As the substitution degree is raised, the saturation magnetization at 4.2 K decreases and the Curie temperature shifts lower, irrespective of the kind of the substituent. That is, the cation substitution yields a reduction of the ferromagnetism. Additionally, both Cr^{3+}- and Co^{3+}-substitution have a large influence on the electrochemical properties. The Cr^{3+}-substitution induces a rise in the average operating potential without a loss of redox capacity, while both the average operating potential and the redox capacity decrease with an increase in the Co^{3+}-substitution degree.

1. Introduction

Rechargeable lithium-ion batteries are state of the art devices and widely applied to cell phones, notebook PCs and electric vehicles. High energy density together with high power performance is required for such batteries, and there are two methods to achieve these characteristics: cell capacity enlargement and operating voltage rise. The utilization of cathode materials which yield high redox potential is an effective way to raise the cell voltage. And from the view point of the cell variety, the utilization of a high-voltage cathode may offer a broader selection of anode materials.

Extensive studies of cation-substituted spinel oxides $LiMn_{2-x}M_xO_4$ (M = Cu^{2+}, Ni^{2+}, Cr^{3+}, Co^{3+}, etc.) have stimulated and extended the possibilities of high-voltage cathode materials [1–6]. Since Zhong et al. first reported that $LiMn_{1.5}Ni_{0.5}O_4$ was capable of Li^+ insertion/extraction around 4.7 V, many experimental works have been presented [2,7–13]. The cathode has a relatively high discharge capacity of 147 mAh g^{-1}, average operating voltage around 4.7 V and good cycle performance. In our previous study, it was found that $LiMn_{1.5}Ni_{0.5}O_4$ had a saturation magnetization of 108 emu g^{-1} at 4.2 K and a Curie temperature of 145 K [9]. Furthermore, the $LiMn_{1.5}Ni_{0.5}O_4$ based spinel cathodes with various surface modifications and partial cation substitutions have been examined to attain a higher operating voltage and good rate capability [14–20].

It is well known that the electrochemical properties strongly depend on the synthesis condition: the difficulty to obtain pure $LiMn_{1.5}Ni_{0.5}O_4$ spinel, where the impurity phase $Li_xNi_{1-x}O$ was found, and two different types of crystal structure, where Ni and Mn ions are randomly located within the 16d site (space group *Fd3m*) or ordered regularly (*P4₃32*) [11–14,21]. It has been proposed that both the impurity phase and the ordered phase trigger electrochemical performance deteriorations in areas such as capacity loss and cycle performance [11,13,22]. The appearance of a 4.0 V redox signal, which is attributed to the Mn^{3+}/Mn^{4+} redox reaction, is brought about by the lowering of the average operating voltage. Various cation substitutions have been tried in order to overcome these problems [15–18]. However, the 4 V redox signal was still observed in most of the previous studies. In this work, we have tried to synthesize pure spinel phase with no redox signal around the 4 V range in the cation-substituted $LiMn_{1.5}Ni_{0.5}O_4$ spinel, where Co^{3+} and Cr^{3+} were selected as the substituent because of their octahedral site preference. Both the low-temperature magnetic property and the electrochemical properties are discussed.

2. Experimental

$LiMn_{1.5-x}M_{2x}Ni_{0.5-x}O_4$ (M = Co or Cr, $0.0 \le x \le 0.2$) particles were synthesized by the sol–gel method. Reagent grade $LiNO_3$, $Mn(CH_3COO)_2{\cdot}4H_2O$, $Ni(CH_3COO)_2{\cdot}4H_2O$, $Cr(CH_3COO)_3$ and $Co(CH_3COO)_2{\cdot}4H_2O$ were used as starting materials. Citric acid

* Corresponding author. Tel.: +81 792 67 4867; fax: +81 792 67 4855.
E-mail address: tatsuya@eng.u-hyogo.ac.jp (T. Nakamura).

0378-7753/$ – see front matter © 2010 Elsevier B.V. All rights reserved.
doi:10.1016/j.jpowsour.2010.11.018

monohydrate $C_6H_8O_7{\cdot}H_2O$ was utilized as a complexing agent. The stoichiometric amounts of the metal acetates were dissolved in distilled water and 1% excess amount of Li nitrate was added in order to compensate for the Li evaporation loss during the annealing process. Finally citric acid was also added, where the molar ratio of metal ions to citric acid was adjusted to 3:1. This solution was evaporated at 70 °C using a rotary evaporator until a viscous transparent gel was obtained. The obtained gel precursors were thermally decomposed at 400 °C in air for 4 h, finely ground and press-compacted into pellets (30 mm in diameter and 4 mm in thickness) at a pressure of approximately 500 kg cm^{-2}. The pellets were annealed at a temperature range of 650–700 °C for 10 h under an oxygen flow, followed by furnace cooling down to room temperature. The annealing temperature was fixed at 650 and 700 °C in the case of Co^{3+}- and Cr^{3+}-substitution, respectively.

The powder X-ray diffraction patterns were measured by a Rigaku RINT-1500 diffractometer with Cu K_α radiation at 4.0 kV and 200 mA. The full diffraction patterns of the products were taken in the 2θ range from 10° to 120° in 0.02° steps to identify the generated phases. The Rietveld refinement (RIETAN 2000 [23]) was carried out in order to obtain the structural parameters. Magnetization of the specimens was measured using a magnetic balance (Shimazu, Magnetic balance, the applied magnetic field less than 10 kOe) with a heating process in the temperature region from 4.2 to 295 K. The electrochemical performances were evaluated with a Li coin cell, which was assembled in an Ar-filled glove box. The active material (20 mg) was mixed thoroughly with acetylene black (5 mg) and polytetrafluoroethylene (PTFE) binder (1 mg), shaped into pellet form, pressed to 13-mm diameter circular Al mesh collector and used as the cathode electrode. 1.0 M $LiPF_6$ in ethylene carbonate–dimethyl carbonate solution (3:7, by vol.) and Li foil were used as the organic electrolyte and anode electrode, respectively. The cells were subjected to galvanostatic cycling in the voltage region from 3.5 to 5.0 V at a constant current of 30 mA g^{-1} (C/5) at room temperature using a program-controlled charge/discharge apparatus (HOKUTO DENKO, HJ1001SM8A).

3. Results and discussion

All the specimens were identified as a single phase cubic spinel oxide with *Fd3m* space group, because the powder X-ray diffraction patterns did not show super structure lines related to the cation ordering nor impurity phases, irrespective of the substitution degree and the kind of the substituent [13]. The refined lattice constant is shown as the substitution degree in Fig. 1(a). The lattice constant increased from 8.172 Å to 8.180 Å with an increase in the Cr^{3+}-substitution degree, while it decreased from 8.172 Å to 8.136 Å with an increase in the Co^{3+}-substitution degree. These variations are attributed to the ionic radius differences among Cr^{3+} (0.76 Å), Co^{3+} (0.69 Å), Mn^{4+} (0.67 Å) and Ni^{2+} (0.83 Å) [24]. In both the Cr^{3+}- and Co^{3+}-substitution case, the variation of the lattice constant was almost linear, implying conformity with Vegard's law. This indicates the formation of a homogeneous solid solution: both the Cr^{3+}- and Co^{3+}-substitutents are uniformly distributed in the spinel compounds.

However, only for the Co^{3+}-substitution degree, it is found that the (2 2 0) diffraction peak was intensified with the substitution degree. The growth of the (2 2 0) diffraction peak means that a certain amount of the transition metal ions were located on the 8a site. The occupancy of transition metal ions on the 8a site is plotted in Fig. 1(b). The amount increased up to 7% with the Co^{3+}-substitution degree, and the Co^{3+}-substitution facilitates the cation mixing between the 8a and 16d sites. On the other hand, for the $LiMn_{1.5-x}Cr_{2x}Ni_{0.5-x}O_4$, the amount of transition metal ions on the 8a site was independent of the substitution degree and less than 2%. According to the crystal-field stabilization, both Ni^{2+} and Mn^{4+} ions have a strong tendency toward the 16d site, while both Cr^{3+} and Co^{3+} have a 16d octahedral preference. Hence, it is likely that all Li^+ is located on 8a site in both $LiMn_{1.5-x}Cr_{2x}Ni_{0.5-x}O_4$ and $LiMn_{1.5-x}Co_{2x}Ni_{0.5-x}O_4$. However, the experimental fact about the Co^{3+}-substitution is inconsistent with the above expectation. There is a possibility that a part of the Co^{3+} ions may be reduced to Co^{2+} ions and introduced on to 8a site [24], but more detailed studies are required to confirm this discussion.

Next, the magnetic properties of $LiMn_{1.5-x}Cr_{2x}Ni_{0.5-x}O_4$ and $LiMn_{1.5-x}Co_{2x}Ni_{0.5-x}O_4$ are discussed. The temperature dependence of the magnetization at $H = 10$ kOe is shown in Fig. 2. The magnetization rapidly increased at a temperature lower than 150 K, implying the presence of a ferromagnetic phase transition. It is well known that the non-substituted $LiMn_{1.5}Ni_{0.5}O_4$ is a ferrimagnetic material with a Curie temperature of 145 K and saturation magnetization of 105 emu g^{-1} at 4.2 K [9]. The magnetic transition temperature was estimated using the Arrot plot technique, and the saturation magnetization at 4.2 K was numerically evaluated with the law of approach to saturation [25,26]. It is clear from Fig. 3(a) that the Curie temperature trended lower with an increase in both Cr^{3+}- and Co^{3+}-substitution. It varied monotonically from 130 to 42 K in the Co^{3+}-substitution case and from 130 to 57 K in the Cr^{3+}-substitution case. These variations are attributed to the super-exchange interaction of transition metal ions, most of which are located on the 16d octahedral site, in the compounds. According to the Kanamori–Goodenough rules of exchange interaction with a bonding angle close to $\pi/2$, both Mn^{4+}–O–Mn^{4+} and Ni^{2+}–O–Ni^{2+} are ferromagnetic and Mn^{4+}–O–Ni^{2+} is an antiferromagnetic coupling [27,28]. Therefore, the ferrimagnetic collinear-spin arrangement is attained in

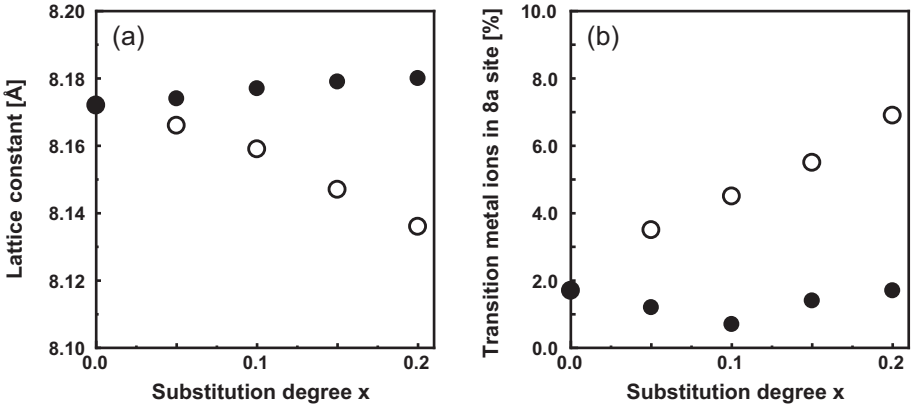

Fig. 1. Variation of (a) the lattice constant and (b) the occupancy of transition metal ions at 8a site with the substitution degree for $LiMn_{1.5-x}M_{2x}Ni_{0.5-x}O_4$: M = Cr (solid circle) and Co (open circle).

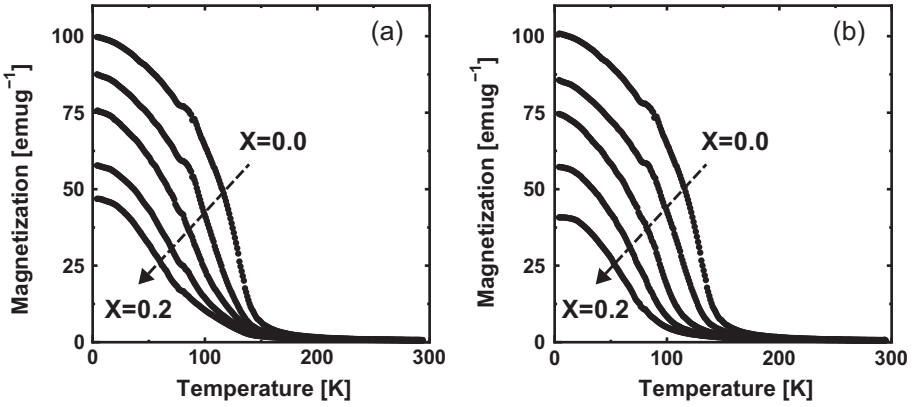

Fig. 2. Temperature variation of magnetization for (a) $LiMn_{1.5-x}Cr_{2x}Ni_{0.5-x}O_4$ and (b) $LiMn_{1.5-x}Co_{2x}Ni_{0.5-x}O_4$ compounds. The applied magnetic field is 10 kOe.

$LiMn_{1.5}Ni_{0.5}O_4$. For the Cr^{3+}-substituted spinels, the following new interactions are introduced into the spinel system: antiferromagnetic couplings of Cr^{3+}–O–Mn^{4+} and Cr^{3+}–O–Ni^{2+}, and a ferromagnetic Cr^{3+}–O–Cr^{3+} coupling. They can break the ferrimagnetic arrangement and introduce magnetic frustration. It is possible to explain the lowering of the Curie temperature with these considerations. On the other hand, the Co^{3+}-substitution simply brings about magnetic dilution due to the diamagnetic Co^{3+} ions. The discontinuity of magnetic percolation may yield a much lower transition temperature, but a small amount of Co^{2+} ions located on the 8a site creates a new super-exchange path between cations on the 8a and 16d sites via a bonding angle of π. It is well known that this new exchange coupling is much stronger than the exchange coupling with a bonding angle of π/2. Consequently, a larger lowering of the Curie temperature is realized.

Fig. 3(b) exhibits the variation of the saturation magnetization with the substitution degree. The saturation magnetization decreased (from 101 to 45 emu g^{-1}) with an increase in the substitution degree, and the values were almost independent of the kind of the substituent. The magnetic frustration with the Cr^{3+}-substitution, as well as the magnetic dilution with the diamagnetic Co^{3+}-substitution, inhibit the ferromagnetic alignment and reduce the saturation magnetization.

There were noticeable differences on the electrochemical properties among the Cr^{3+}- and Co^{3+}-substitutions. Fig. 4 shows typical dQ/dV curves, which were numerically derived from the potential profiles obtained by the electrochemical cell using $LiMn_{1.5-x}Cr_{2x}Ni_{0.5-x}O_4$ and $LiMn_{1.5-x}Co_{2x}Ni_{0.5-x}O_4$ cathodes. In the initial charging process, the electrochemical system was largely influenced by some irreversibility such as the decomposition of the electrolyte. Therefore, the curves were obtained on the initial discharging process and subsequent cycles. For all specimens, no redox signal was observed around 4.0 V, which is related to the redox reaction of Mn^{3+}/Mn^{4+} [12,14]. It implied that the specimens are almost stoichiometric compounds and free of oxygen vacancies. For the cathode with $x = 0.0$, two narrow and well-resolved peaks were observed on both the charge and discharge curves around 4.7 V. They were located at 4.73 and 4.77 V on the charging process, and correspond to the reversible oxidation/reduction of Ni^{2+}/Ni^{3+} and Ni^{3+}/Ni^{4+} redox couples, respectively [16,21]. It is clear from the viewgraph that both Cr^{3+}- and Co^{3+}-substitution led to the broadening of the redox current peaks. It is thought that the redox signals of Cr^{3+}/Cr^{4+} or Co^{3+}/Co^{4+} is superimposed to the twin Ni^{2+}/Ni^{3+} and Ni^{3+}/Ni^{4+} signals. In the Cr^{3+}-substitution case, the peak corresponding to the Ni^{3+}/Ni^{4+} redox couple shifted higher on both the charging and discharging processes. The peak positions of the Ni^{2+}/Ni^{3+} redox couple remained unchanged and a new peak appeared at 4.94 and 4.87 V on the charging and discharging process, respectively, which are thought to be related to the Cr^{3+}/Cr^{4+} redox reaction. The redox voltage differences of the Ni^{2+}/Ni^{3+} and Ni^{3+}/Ni^{4+} signals remained almost unchanged. On the other hand, the Co^{3+}-substitution brought about the following modifications: the lowering of the Ni^{2+}/Ni^{3+} redox couple on both the charging and discharging processes, and the rising of the Ni^{3+}/Ni^{4+} redox couple on the discharging process. Consequently, the redox peak separation of Ni^{3+}/Ni^{4+} grew with the substitution, implying an increase in polarization.

Fig. 5 shows the variation of the initial discharge capacity vs. the substitution degree in the $LiMn_{1.5-x}Cr_{2x}Ni_{0.5-x}O_4$ and $LiMn_{1.5-x}Co_{2x}Ni_{0.5-x}O_4$ cathodes. It is clearly seen that the capacity

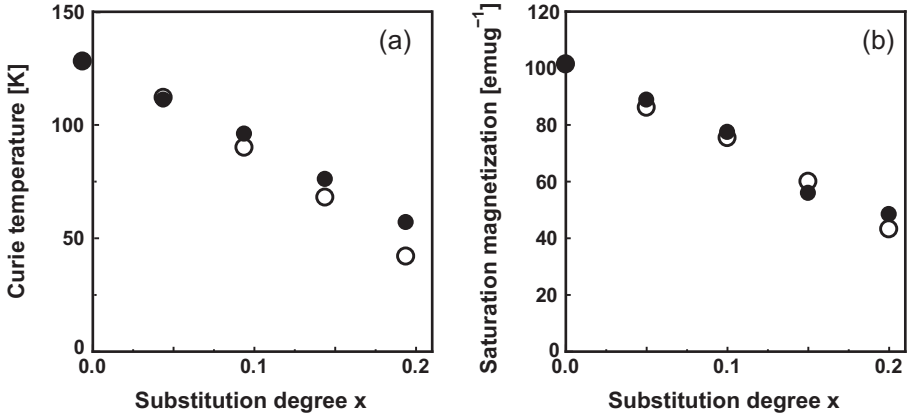

Fig. 3. (a) Curie temperature and (b) saturation magnetization at 4.2 K vs. the substitution degree for $LiMn_{1.5-x}M_{2x}Ni_{0.5-x}O_4$: M = Cr (solid circle) and Co (open circle).

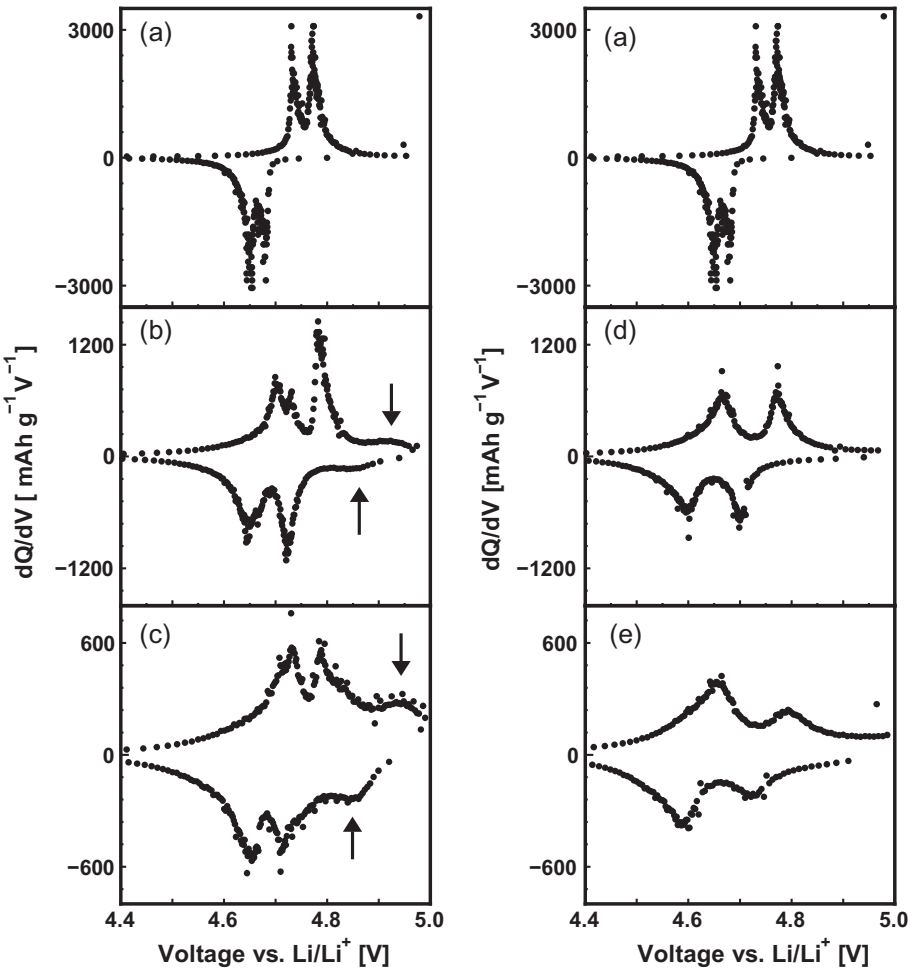

Fig. 4. dQ/dV curves of the 2nd charge and discharge process for $LiMn_{1.5-x}Cr_{2x}Ni_{0.5-x}O_4$ (x = 0.0 (a), x = 0.1 (b) and x = 0.2 (c)) and $LiMn_{1.5-x}Co_{2x}Ni_{0.5-x}O_4$ (x = 0.0 (a), x = 0.1 (d) and x = 0.2 (e)) cathodes. The cells were cycled in the voltage range 3.5–5.0 V at room temperature. The current rate was C/5. Newly appeared peaks are indicated with arrows.

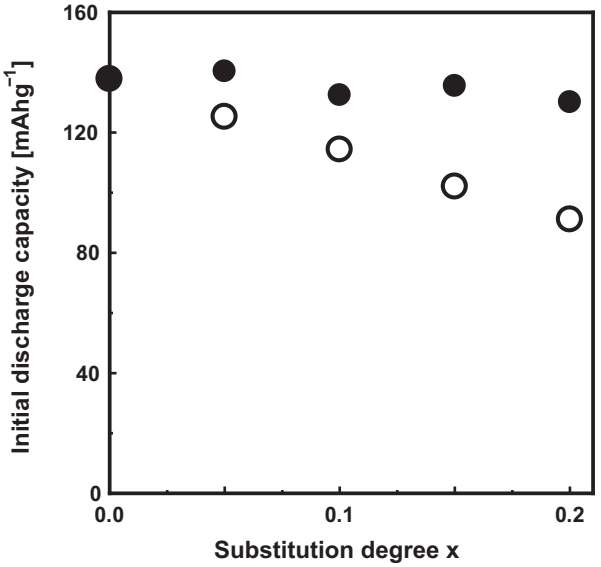

Fig. 5. Variation of the initial discharge capacity with the substitution degree for $LiMn_{1.5-x}M_{2x}Ni_{0.5-x}O_4$: M = Cr (solid circle) and Co (open circle).

of the $LiMn_{1.5-x}Cr_{2x}Ni_{0.5-x}O_4$ cathodes only slightly decreased with an increase in the Cr^{3+}-substitution degree. By contrast, with an increase in the Co^{3+} content for $LiMn_{1.5-x}Co_{2x}Ni_{0.5-x}O_4$, the capacity decreased from 138 mAh g^{-1} for x = 0.0 to 91 mAh g^{-1} for x = 0.2. Several researchers also reported this capacity reduction of Co^{3+}-substituted Li–Mn–Ni spinel [17,18]. Considering the above structural analysis, it is likely that the capacity reduction is attributed to the cation mixing: Co^{2+} on the 8a site cannot contribute to the electrochemical reaction. Further, the growth of the redox potential separation in Co^{3+}-substituted spinel also degrades the redox reversibility, resulting in a lowering of the capacity. On the other hand, it was clear from Table 1 that the capacity retention after the

Table 1
Discharge capacities at 1st and 20th cycles of $LiMn_{1.5-x}Cr_{2x}Ni_{0.5-x}O_4$ and $LiMn_{1.5-x}Co_{2x}Ni_{0.5-x}O_4$ cathodes.

Sample	Capacity [mAh g^{-1}] (1st cycle/20th cycle)
$LiMn_{1.5}Ni_{0.5}O_4$	137.8/123.9
$LiMn_{1.45}Cr_{0.1}Ni_{0.45}O_4$	140.4/134.1
$LiMn_{1.4}Cr_{0.2}Ni_{0.4}O_4$	132.5/127.4
$LiMn_{1.35}Cr_{0.3}Ni_{0.35}O_4$	139.7/131.4
$LiMn_{1.3}Cr_{0.4}Ni_{0.3}O_4$	130.1/118.0
$LiMn_{1.45}Co_{0.1}Ni_{0.45}O_4$	125.2/118.8
$LiMn_{1.4}Co_{0.2}Ni_{0.4}O_4$	116.4/110.3
$LiMn_{1.35}Co_{0.3}Ni_{0.35}O_4$	105.8/103.1
$LiMn_{1.3}Co_{0.4}Ni_{0.3}O_4$	97.7/94.8

20th cycle was always greater than 90%, irrespective of the kind and amount of the substituents. For example, the $LiMn_{1.4}Cr_{0.2}Ni_{0.4}O_4$ and $LiMn_{1.4}Co_{0.2}Ni_{0.4}O_4$ cathodes showed good capacity retention of 96% and 95% after 20th cycle. This experimental fact implies that a small amount of cation mixing has relatively little influence on the reversibility of Li^+ intercalation/de-intercalation in the spinel cathode. It is thought to be related to the fact that the spinel framework has a three-dimensional lithium diffusion path [14], while the two-dimensional migration in layered rock-salt compounds may be easily disturbed with the cation mixing.

4. Conclusion

The magnetic and electrochemical properties of $LiMn_{1.5-x}M_{2x}Ni_{0.5-x}O_4$ (M = Co or Cr, $0.0 \leq x \leq 0.2$) were studied with DC magnetic measurement and galvanostatic charging/discharging. It was found from XRD analysis that single phase cubic spinel oxide was obtained for both substitution systems and the cation mixing between 8a and 16d sites occurred in the Co^{3+}-substitution compound. The magnetic ordering degree was decreased in both substitution systems, and attributed to the magnetic frustration within the 16d site in the Cr^{3+}-substitution compound and the magnetic dilution of diamagnetic ions in the Co^{3+}-substitution compound. The electrochemical properties were also greatly influenced by the cation substitutions. Regarding the cycle performances, there were little differences between both substitution systems and the capacity loss on the redox cycling was less significant. The Cr^{3+}-substitution led to higher operating voltage with no sacrifice of the discharge capacity. On the other hand, the Co^{3+}-substitution caused the lowering of the operating voltage with a capacity loss. Consequently, the utilization of the Cr^{3+}-substituted cathode enlarged the energy density of the battery cell.

References

[1] Y. Ein-Eli, W.F. Howard Jr., S.H. Lu, S. Mukerjee, J. McBreen, J.T. Vaughey, M.M. Thackeray, J. Electrochem. Soc. 145 (1998) 1238.
[2] Q.M. Zhong, A. Bonakdarpour, M.J. Zhang, Y. Gao, J.R. Dahn, J. Electrochem. Soc. 144 (1997) 205.
[3] C. Sigala, D. Guyomard, A. Verbaere, Y. Piffard, M. Tournoux, Solid State Ionics 81 (1995) 167.
[4] H. Kawai, M. Nagata, H. Tukamoto, A.R. West, Electrochem. Solid State Lett. 1 (1998) 212.
[5] H. Kawai, M. Nagata, M. Kageyama, H. Tukamoto, A.R. West, Electrochem. Acta 45 (1999) 315.
[6] H. Shigemura, M. Tabuchi, H. Kobayashi, A. Hirano, H. Kageyama, J. Mater. Chem. 12 (2002) 1882.
[7] T. Ohzuku, S. Takeda, M. Iwanaga, J. Power Sources 81–82 (1999) 90.
[8] K. Kanamura, W. Hoshikawa, T. Umegaki, J. Electrochem. Soc. 149 (2002) A339.
[9] T. Nakamura, Y. Yamada, M. Tabuchi, J. Appl. Phys. 98 (2005) 093905.
[10] K. Amine, H. Tukamoto, H. Yasuda, Y. Fujita, J. Power Sources 68 (1997) 604.
[11] K. Amine, H. Tukamoto, H. Yasuda, Y. Fujita, J. Electrochem. Soc. 143 (1996) 1607.
[12] H. Duncan, Y. Abu-Lebdeh, I.J. Davidson, J. Electrochem. Soc. 157 (2010) A528.
[13] D. Liu, J. Han, J.B. Goodenough, J. Power Sources 195 (2010) 2918.
[14] R. Santhanam, B. Rambabu, J. Power Sources 195 (2010) 5442.
[15] M. Aklalouch, J.M. Amarilla, R.M. Rojas, I. Saadoune, J.M. Rojo, J. Power Sources 185 (2008) 501.
[16] M. Aklalouch, R.M. Rojas, J.M. Rojo, I. Saadoune, J.M. Amarilla, Electrochem. Acta 54 (2009) 7542.
[17] A. Ito, D. Li, Y. Lee, K. Kobayakawa, Y. Sato, J. Power Sources 185 (2008) 1429.
[18] R.M. Rojas, J.M. Amarilla, L. Pascual, J.M. Rojo, D. Kovacheva, K. Petrov, J. Power Sources 160 (2006) 529.
[19] M. Aklalouch, J.M. Amarilla, R.M. Rojas, I. Saadoune, J.M. Rojo, Electrochem. Commun. 12 (2010) 548.
[20] T.A. Arunkumar, A. Manthiram, Electrochem. Solid State Lett. 8 (2005) A403.
[21] X. Fang, N. Ding, X.Y. Feng, Y. Lu, C.H. Chen, Electrochem. Acta 54 (2009) 7471.
[22] J.H. Kim, S.T. Myung, C.S. Yoon, S.G. Kang, Y.K. Sun, Chem. Mater. 16 (2004) 906.
[23] F. Izumi, T. Ikeda, Mater. Sci. Forum 198 (2000) 321.
[24] R.D. Shannon, Acta Crystallogr. A A32 (1976) 751.
[25] A. Arrot, Phys. Rev. 108 (1957) 1394.
[26] S. Chikazumi, Physics of Magnetism, John Wiley and Sons Inc., New York, 1964, p. 276.
[27] J. Kanamori, J. Phys. Chem. Solids 10 (1959) 87.
[28] J.B. Goodenough, Magnetism and the Chemical Bond, Wiley, New York, 1963.